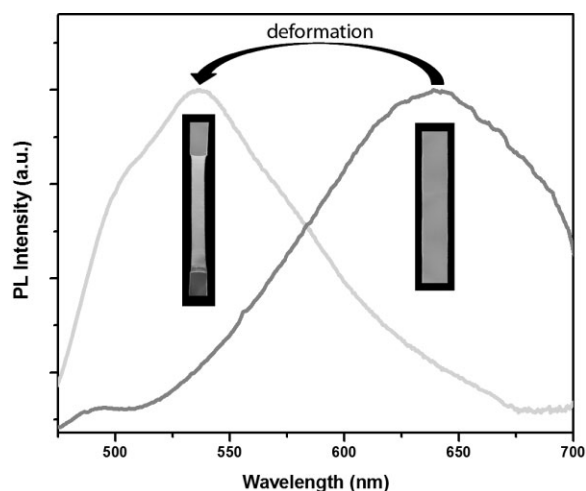


# Luminescent Mechanochromic Sensors Based on Poly(vinylidene fluoride) and Excimer-Forming *p*-Phenylene Vinylene Dyes<sup>a</sup>

Joseph Lott, Christoph Weder\*

Cyano-substituted excimer-forming oligo(phenylene vinylene) dyes (cyano-OPVs) with terminal alkyl tails of different length were blended with two fluorinated host polymers with similar chemical composition but differing crystallinity. These blends were used to fabricate luminogenic mechanochromic thin films, which change their emission color upon deformation. The alkyl tails affect the solubility of the chromophores in the polymer matrix and lead to different aggregation properties; this is of importance because the mechanochromic fluorescence color change of the blends is related to the self-assembly of the excimer-forming dye in the unperturbed polymer matrix, and the dispersion of the dye aggregates upon deformation. Besides the length of the solubilizing tails, the dye concentration has an important influence on the aggregate size, which is crucial to creating a mechanochromic response, since the dye aggregates must be small enough to be dispersed during the deformation process. In-situ opto-mechanical measurements have shown that the mechanochromic effect occurs primarily during plastic deformation and that the mechanically induced dispersion of the dye aggregates becomes more pronounced as the crystallinity of the matrix polymer increases.



## Introduction

Fueled by academic curiosity and the potential for use in applications that range from security features,<sup>[1]</sup> light-emitting diodes,<sup>[2]</sup> lasers,<sup>[3]</sup> to chemical sensors,<sup>[4]</sup> the development of luminogenic polymers<sup>[5]</sup> is attracting much interest in laboratories around the world. We recently developed a new family of stimuli-responsive luminogenic polymers, which change their emission color upon exposure to a range of stimuli.<sup>[6]</sup> These materials are produced by incorporating small amounts of excimer-forming sensor dyes into a variety of host polymers. In most cases this can be achieved by creating physical blends of the

C. Weder

Adolphe Merkle Institute and Fribourg Center for Nanomaterials,  
University of Fribourg, CH-1700 Fribourg, Switzerland

Fax: (+41) 26 300 96 24; E-mail: christoph.weder@unifr.ch

J. Lott, C. Weder

Department of Macromolecular Science and Engineering and  
Center for Layered Polymeric Systems, Case Western Reserve  
University, Cleveland, Ohio 44106, USA

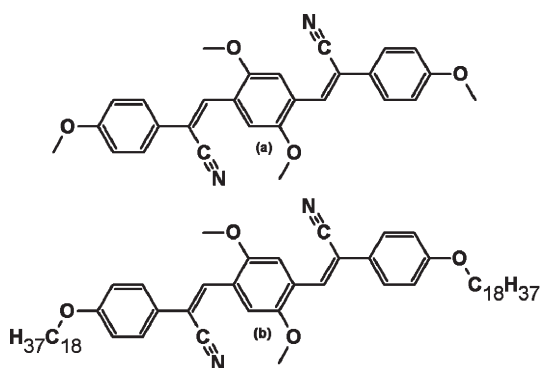


**Figure 1.** Chemical structures of the two cyano-OPV chromophores used in this study (a) C1-RG and (b) C18-RG.

dye and the host polymer by conventional melt-processing techniques. The approach exploits the excimer-forming properties of chromophores such as cyano-substituted oligo(phenylene vinylene)s<sup>[7–12]</sup> (cyano-OPVs, Figure 1) and further relies on the stimulus-driven self-assembly or dispersion of nano-scale aggregates of these sensor dyes in a range of host polymers. We have shown that this general concept of stimulus-triggered dye (dis)assembly in polymer matrices allows for the design of a broad range of sensor materials, which are useful for the detection of temperature history,<sup>[13–17]</sup> exposure to chemicals,<sup>[18,19]</sup> and mechanical deformation,<sup>[20–24]</sup> as well as more complex combinations of stimuli, such as seen in shape-memory materials.<sup>[25]</sup> Others have adapted the concept and extended it to a range of dyes including cyano containing poly(phenylene ethynyls),<sup>[26]</sup> perylenes,<sup>[27]</sup> CdS nanoparticles,<sup>[28]</sup> and bis(benzoxazolyl)stilbenes.<sup>[29]</sup>

The temperature and humidity sensors based on such polymer/dye blends operate by kinetically trapping a thermodynamically unstable molecular mixture of the components by rapidly cooling a hot (and at this temperature miscible) mixture below its glass transition temperature ( $T_g$ ).<sup>[13,19]</sup> If the material is subsequently heated above  $T_g$ , the system becomes sufficiently mobile to equilibrate, resulting in aggregation of the dye molecules and the formation of excimers. This approach yields time-temperature indicating materials that exhibit a pronounced fluorescence color change, whose kinetics follow a predictable, Arrhenius-type behavior.<sup>[14–17]</sup> For humidity sensors, a hygroscopic host polymer is chosen, which has a  $T_g$  that is above the desired working temperature.<sup>[18]</sup> Moisture serves to plasticize the matrix thus lowering  $T_g$  and providing the mobility to facilitate the aggregation process. The same concept can be applied to detect other chemical stimuli.<sup>[19]</sup>

The mechanically responsive systems based on this framework rely on the inverse mechanism, namely the dispersion of nano-scale dye aggregates upon deformation

of the material. Systematically investigating several model systems, including polyolefins,<sup>[14,20–23]</sup> polyurethanes,<sup>[22]</sup> and polyesters,<sup>[14,15,25]</sup> we explored how the nature of the polymer, dye concentration and solubility in the host polymer, dye aggregate size, and effectiveness of the dye aggregate break-up influence the mechanochromic response of such materials. The dye concentration in the material must be sufficiently high to cause aggregation of dye molecules and lead to the formation of static excimers. Appropriate (in)solubility of the dyes in a particular matrix polymer can be tailored by changing the nature of the substituents attached to the dye core, e.g., the length of (aliphatic) solubilizing groups.<sup>[15]</sup> Using a series of polyethylenes (PEs) of different crystallinity, and the two dyes 1,4-bis( $\alpha$ -cyano-4-methoxystyryl)-2,5-dimethoxybenzene (C1-RG, Figure 1) and 1,4-bis( $\alpha$ -cyano-4-octadecyloxystyryl)-2,5-dimethoxybenzene (C18-RG, Figure 1) we demonstrated that the formation of small dye aggregates is important for efficient mechanochromic systems, since large-scale phase separation limits or prevents the break-up of the dye aggregates upon deformation.<sup>[23]</sup> The rate at which C1-RG aggregates, the aggregate size, and the extent of aggregation were found to decrease with increase in polymer crystallinity.<sup>[23]</sup> This observation is in agreement with the well-established decrease of the fractional free volume of the non-crystalline component of PE with increasing crystallinity and reflects a decrease in the dye's translational mobility. While in linear low-density PE of moderately high density ( $0.94 \text{ g} \cdot \text{cm}^{-3}$ ) the aggregation of C1-RG can (at room temperature) last several months,<sup>[21]</sup> dye aggregation and excimer formation was found to be virtually instantaneous in a range of different PE grades comprising C18-RG.<sup>[23]</sup> Together with the fact that in similarly processed PE samples C18-RG formed much smaller aggregates than C1-RG, it appears that the nucleation of C18-RG is much faster than that of C1-RG, leading to the rapid growth of smaller aggregates, which are more easily dispersed upon deformation than those of C1-RG and result in a more substantial photoluminescence (PL) emission color change.<sup>[23]</sup> In situ opto-mechanical experiments have shown that the PL color change of blends upon deformation matches nicely with the shape of the stress-strain profiles for the samples. Blend films based on several different PE matrices exhibit a steep increase in color change upon yielding, an only moderate increase during neck propagation, and a slightly steeper increase during strain hardening. It was also shown that the magnitude of the PL color change, and therewith the extent of aggregate break-up increases with decrease in strain rate. Investigation of the effect of polymer crystallinity on the mechanochromic response of PE/C18-RG blends revealed a larger extent of color change upon deformation for the higher crystallinity PEs. From a mechanistic aspect, it appears that the ability of the polymer host to disperse dye aggregates

upon deformation is primarily related to the plastic deformation process of the PE crystallites.<sup>[23]</sup> These findings are consistent with the mechanochromic response of several polyesters that have also been investigated.<sup>[15,24]</sup>

With the objective of broadening our understanding for the mechanistic aspects of dye-aggregate (de)formation in semicrystalline host polymers, and also with the significant technological importance of thermoplastic fluoropolymers in mind (which are used in applications that range from fishing lines to insulation for electrical wires<sup>[30]</sup>), we have chosen to study the mechanochromic response of blends of C1-RG and C-18RG in polyfluorinated host polymers of different crystallinity.

## Experimental Part

### Materials

The chromophores C1-RG<sup>[31]</sup> and C18-RG<sup>[15]</sup> were synthesized as previously described. Poly(vinylidene fluoride) (PVDF) was purchased from Aldrich (weight-average molecular weight,  $M_w = 530\,000$ ) and poly[(vinylidene fluoride)-*co*-(hexafluoropropylene)] (PVDF-HFP) was obtained from Solvay (Solef TA 21508); these polymers were used as received.

### Sample Preparation

Blends comprised of one of the dyes and one of the polymers were prepared using a DACA lab-scale, co-rotating twin-screw extruder, which was operated at 210 °C and 100 rpm. The composition of the blends was controlled by feeding the desired amounts of chromophore and polymer into the extruder and mixing was accomplished by re-cycling the mixture through the instrument for 5 min before the product was extruded from the machine. Thin films of a thickness of  $\approx 175\ \mu\text{m}$  were prepared from the extrudates using a Carver melt press, pressing at 230 °C at 4 tons for 3 min between Kapton sheets, using aluminum spacers to control the film thickness. Upon removal from the press, films were immediately immersed in an ice water bath and the films thus quenched were allowed to age for at least 3 weeks under ambient conditions before further use. For mechanical testing, rectangular strips (dimensions 15 mm  $\times$  6 mm) were cut and notched with a 5/8 inch. round stencil on both sides, to create a dog-bone like structure with a minimum gap distance of 2 mm between the round notches.<sup>[23]</sup>

### Fluorescence Microscopy

Fluorescence microscopy images were collected on a Leica DMI 6000 B inverted microscope (Leica Microsystems Wetzlar, Germany) with a 40 $\times$  objective (N PLAN N.A. = 0.55) using a Retiga camera (Q-imaging Vancouver British Columbia). The resulting magnification is 400 $\times$ . Samples were illuminated using an excitation wavelength of 340–380 nm with a dichroic mirror at 400 nm; on the detection side, a long pass emission filter at 425 nm was used.

### Photoluminescence (PL) Spectroscopy

Steady-state PL spectra were collected using a Photon Technology International QuantaMaster 40 spectrophotometer under excitation at 430.5 nm; the spectra were corrected for instrument throughput and detector response. For opto-mechanical studies, PL spectra were recorded using an Ocean Optics ACD1000-USB spectrometer under excitation at 377 nm; these spectra were not corrected. On the latter system, the excitation wavelength of 377 nm was dictated by the use of an LED with fixed wavelength. On the former, excitation at 430.5 nm was chosen with the objective to excite at the wavelength of maximum absorption to maximize the signal intensity. The different excitation wavelengths affect the emission spectra only in that their overall intensity changes, but the spectral shapes and peak positions are not changed.

### Opto-Mechanical Experiments

Ex-situ opto-mechanical studies were carried out by first uniaxially deforming the samples on a homebuilt stretching frame and subsequent measurement using the Ocean Optics spectrophotometer mentioned above. In-situ opto-mechanical studies were carried out using the Ocean Optics spectrometer in conjunction with an Instron 5565 mechanical testing frame using a 1 kN load cell. All samples were deformed at a rate of 1.0 mm  $\cdot$  min<sup>-1</sup>. The local strain was calculated by measuring the displacement of two ink marks located 2 mm on either side of the center of the notch.

## Results and Discussion

For this study, we elected to employ the cyano-OPVs C1-RG and C18-RG, which were already used in our previous work on mechanochromic PEs (vide supra) and whose chemical structures are shown in Figure 1. These chromophores have identical conjugated cores and therefore exhibit virtually identical absorption ( $\lambda_{\text{max}} \approx 434\text{--}437\ \text{nm}$ ) and monomer-dominated emission ( $\lambda_{\text{max}} \approx 506\ \text{and}\ 538\ \text{nm}$ ) properties in dilute  $\text{CHCl}_3$  solution.<sup>[15,21]</sup> Aggregation causes the emission band to broaden and red-shift, e.g., in linear low-density polyethylene (LLDPE) to  $\approx 644\text{--}650\ \text{nm}$ , which is indicative of excimer formation.<sup>[15,21]</sup> While their molecular optical properties are very similar, the chromophores differ in the nature of their terminal solubilizing groups, which change the enthalpic interactions among the dye molecules and with the host polymers, leading to differences in solubility, nucleation characteristics, and self-assembled architecture.<sup>[14,32]</sup> In addition, we chose to examine two different fluorinated host polymers, namely a PVDF homopolymer with a crystallinity of  $\approx 40\%$  (compression-molded films of the neat polymer that were quenched in ice water, see Supporting Information Figure S1a) and a statistical copolymer of PVDF and  $\approx 15\%$  w/w HFP (PVDF-HFP), which displays a much lower crystallinity ( $\approx 20\%$ , same conditions, see Supporting Information Figure S1b).

Binary blends of the polymers and between 0.01 and 0.5% w/w of one of the dye were prepared by melt-mixing the components at 210 °C in a co-rotating twin-screw mini-extruder, compression-molding the resulting blends at 230 °C, and quenching the samples thus produced to obtain films of a thickness of  $\approx 175 \mu\text{m}$  (see Experimental Part for details). The phase behavior of these materials was then screened in a semi-quantitative manner by evaluation of the emission spectra at room temperature. Blends of C18-RG, in either polymer host and regardless of dye concentration (0.01–0.3% w/w), always displayed orange fluorescence and PL spectra with emission maxima around 650 nm (Figure 2). This is consistent with excimer formation as a result of chromophore aggregation and points to an exceedingly low solubility of this dye in the fluoropolymers investigated. Blends of C1-RG at a concentration of 0.1%, in either polymer host, displayed green fluorescence and PL spectra exhibit emission maxima around 535 nm, with only a weak tail into the red regime (Figure 3). This is consistent with predominant monomer emission as a result of a high level of molecular dispersion of this dye and reflects that the solubility of C1-RG in the present fluoropolymers is much higher than that of C18-RG. To further probe the solubility of these dyes in fluorinated hosts, the absorbance and PL spectra of both dyes in two different fluorinated solvents, 2,2,2-trifluoroethanol and hexafluoro-2-propanol were recorded (Figure S2 of Supporting Information). Comparison of the spectra with previously reported data of chloroform solutions<sup>[31]</sup> confirms that in dilute solutions ( $5 \times 10^{-6} \text{ M}$  in trifluoroethanol and  $7 \times 10^{-6} \text{ M}$  in hexafluoro-2-propanol) C1-RG forms molecular solutions (leading to narrow absorption bands with maxima at 414 and 407 nm and green emission with maximum centered around

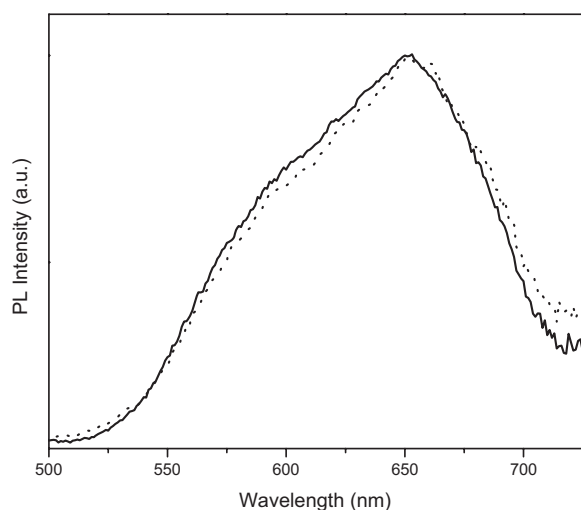


**Figure 2.** Photoluminescence (PL) spectra of blend films consisting of 0.05% w/w C18-RG in PVDF (solid) and 0.1% w/w C18-RG in PVDF-HFP (dotted). The samples were excited at 377 nm and the spectra are normalized so that their maximum intensities match.

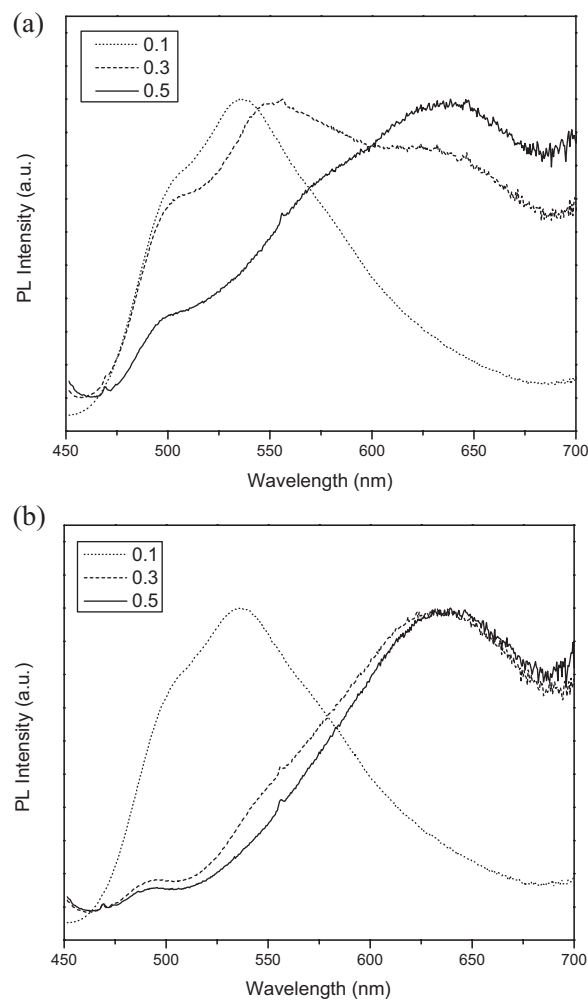


**Figure 3.** Photoluminescence (PL) spectra of blend films consisting of 0.1 (solid), 0.3 (dashed) or 0.5% w/w (dotted) C1-RG in (a) PVDF (b) PVDF-HFP. The samples were excited at 430.5 nm and the spectra are normalized so that their maximum intensities match.

510 nm). By contrast, even at a concentration of  $1 \times 10^{-6} \text{ M}$ , C18-RG forms ground-state aggregates, as evidenced by a characteristic shoulder in the absorption spectra at 520 nm and orange emission with a broad peak centered around 600 nm. These findings support the claim that in the fluorinated polymer hosts investigated, C18-RG displays a much lower solubility than C1-RG and even at low concentration was found to form aggregates.

The orange hue and the relative magnitude of the excimer band centered around 640 nm (Figure 3) increased when the concentration of C1-RG in the blends was raised to 0.3 or 0.5% w/w, indicative of substantial dye aggregation at these concentrations. Unlike the C18-RG-comprising blends, residual monomer emission can be observed in all samples even at a dye concentration of 0.5% w/w. The residual monomer emission is more pronounced in the PVDF homopolymer than the PVDF-HFP copolymer;

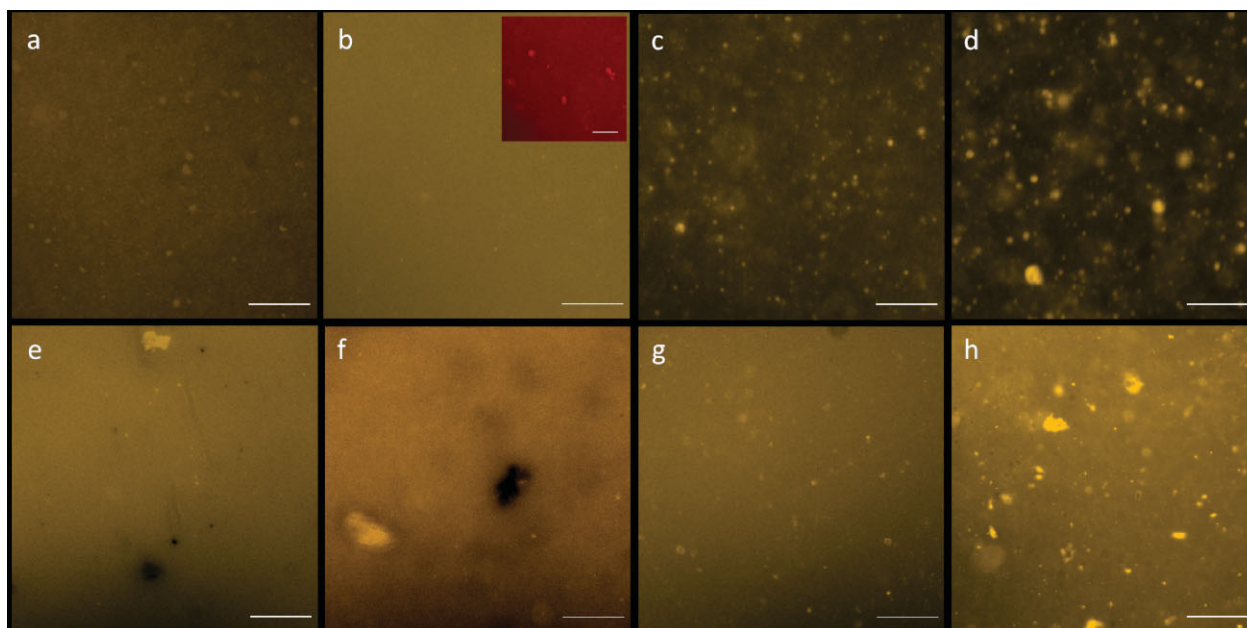


**Figure 4.** Optical micrographs of blend films consisting of C18-RG in (a) PVDF (0.05% w/w) (b) PVDF-HFP (0.01% w/w) (c) PVDF-HFP (0.1% w/w) (d) PVDF-HFP (0.3% w/w) and C18-RG in (e) PVDF (0.3% w/w) (f) PVDF-HFP (0.3% w/w) (g) PVDF (0.5% w/w) (h) PVDF-HFP (0.5% w/w). Images were taken as 12 bit monochrome images and the microscope's software was used to generate pseudocolor images. Inset of (b) was taken as a 24 bit color image. All scale bars represent 20  $\mu\text{m}$ .

suggesting that portions of the chromophore are kinetically trapped in these materials. To probe if and to what extent the emission characteristics of the C18-RG containing blends were influenced by kinetic effects, blend films were treated by annealing at 90 °C for 2 h as well as by immersion in methanol at 25 °C for 48 h. In the case of the 0.1% w/w containing blends, the emission spectra did not change, indicating that at this concentration the dye is indeed thermodynamically soluble in the polymer hosts and not kinetically trapped. For blends of both 0.3 and 0.5% w/w C18-RG in the homopolymer, the relative intensity of the residual monomer emission decreased and the emission shifted toward the excimer peak after immersion in methanol over a period of 48 h indicating that some portion of the chromophores were indeed kinetically trapped.

The emission characteristics of all materials (except for the 0.1% w/w C18-RG blends, which displayed hardly any excimer emission) were investigated as a function of mechanical deformation. Ex situ opto-mechanical studies were carried out by first uniaxially deforming the films to a draw ratio  $\lambda = (l - l_0)/l_0$  of at least 400% ( $l_0, l$  = sample length before and after deformation). Quite interestingly, and in stark contrast to previously investigated polyolefins and polyesters containing this dye,<sup>[14,15,22]</sup> none of the blend films comprising C18-RG displayed any visually appreciable change of the emission color upon deformation (data not shown). This is consistent with the low solubility of this chromophore in the two fluorinated polymers, which might lead to the formation of large aggregates, and which cannot

be efficiently dispersed upon deformation. Figure 4a–d show optical micrographs of C18-RG containing blend films. Indeed, in materials of all concentrations investigated, large dye aggregates ( $\approx 0.5$ – $10 \mu\text{m}$ ) can be seen. This finding seems to suggest that the previously observed formation of nano-scale C18-RG aggregates in PE blends may not primarily be a feature that is intrinsic to the dye, but that polymer-crystal induced nucleation effects may play an important role.

The blend films comprising C18-RG in a concentration of 0.5% w/w displayed a similar non-responsive behavior; the emission color did not change appreciably upon deformation and also in this case, this appears to be related to the formation of large aggregates which are not dispersed upon stretching (Figure 4g, h). PVDF and PVDF-HFP blends comprising C18-RG at a concentration of 0.3% w/w, however, displayed a significant change of the emission characteristics upon uniaxial deformation. Figure 5 shows the emission spectra of films of both materials before and after deformation. A comparison of the spectra makes it evident that the deformation-induced color change is more distinct in the more crystalline PVDF host than in the less crystalline PVDF-HFP copolymer. The deformed PVDF blend shows a sharp green emission band centered at 544 nm and the excimer band around 640 nm has almost completely disappeared after deformation. By contrast, in the PVDF-HFP blend the excimer emission is only partially reduced and the contribution of monomer emission is weak. This pronounced mechanochromic response, particularly for the

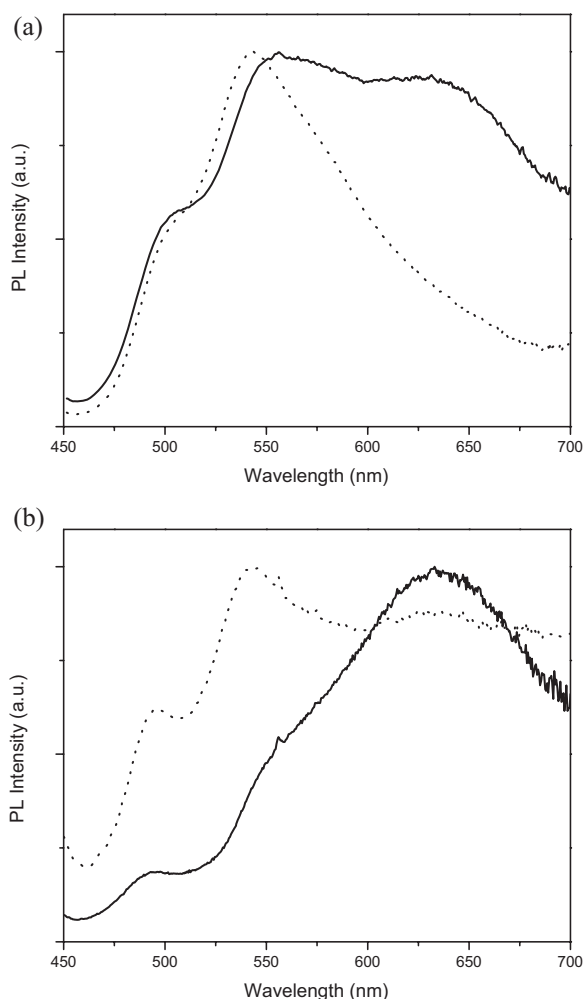


**Figure 5.** Photoluminescence (PL) spectra of blend films consisting of 0.3% w/w C1-RG in (a) PVDF (b) PVDF-HFP before (solid) and after (dotted) stretching the samples to a strain of 100%. The samples were excited at 430.5 nm and the spectra are normalized so that their maximum intensities match.

PVDF-based blend, suggests that this concentration regime allows for appropriate self-assembly of the dye, resulting in dye aggregates of dimensions that are easily dispersed upon plastic deformation. Indeed, Figure 4e, f show a few scattered large scale aggregates; however, the majority of the aggregates seem to be of a size that is below the resolution of the optical microscope.

To elucidate the relationship between deformation and color change in more detail, in situ opto-mechanical experiments were conducted, in which the PL emission from a sample was monitored while performing uniaxial tensile deformation tests. For these experiments, it is convenient and useful to express the PL color by the ratio between the intensities of the monomer and excimer emission ( $I_M/I_E$ ), which were monitored at 546 and 650 nm. The results for the blends comprising 0.3% w/w C1-RG are

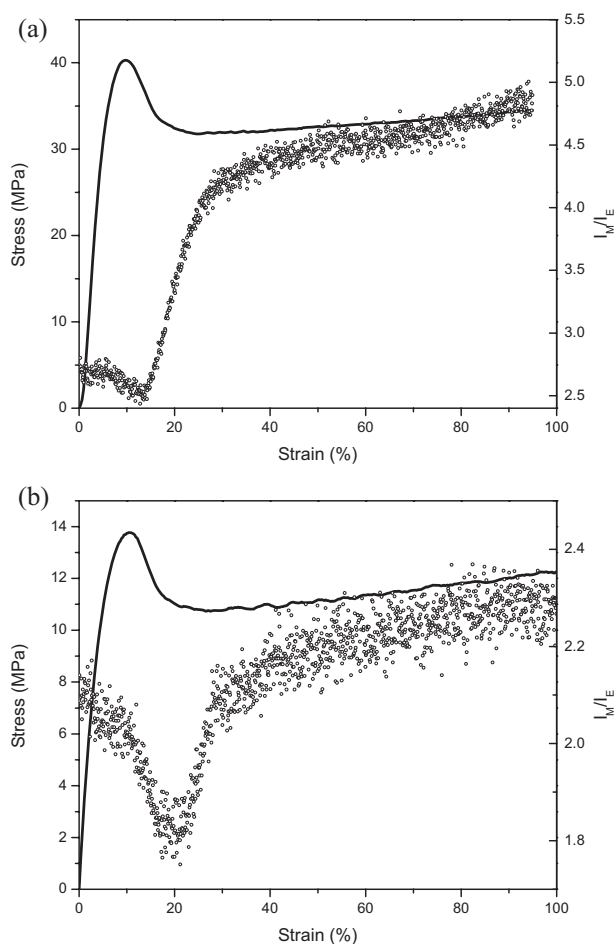


**Figure 6.** Stress (solid) and  $I_M/I_E$  ratio (dotted, measured at 546 and 650 nm) as a function of strain for blend films consisting of 0.3% w/w C1-RG in (a) PVDF and (b) PVDF-HFP.

shown in Figure 6. Both polymer systems show a typical stress–strain response consisting of elastic deformation followed by necking and strain hardening during drawing. The yield strength (40 MPa) and modulus (820 MPa) of the PVDF homopolymer are greater than the values determined for the PVDF-HFP copolymer (14 and 270 MPa, respectively), consistent with the difference in crystallinity. In the case of the PVDF-based blend, the shape of the  $I_M/I_E$ -strain traces displays striking similarities to the stress–strain profile;  $I_M/I_E$  remains unchanged in the elastic regime, is slightly reduced during the onset of neck formation before exhibiting a steep increase upon yielding, increases only moderately during neck propagation, and displays a slightly steeper increase during strain hardening (Figure 6a). For the PVDF-HFP blends, the  $I_M/I_E$ -strain trace has lower absolute values reflecting a higher contribution of excimer emission. However this curve remains unchanged in the elastic regime, is slightly reduced during the onset of neck formation, and rebounds upon yielding.

Interestingly, the overall change in the  $I_M/I_E$  ratio is very small, indicative of insufficient breakup of aggregates. This coincides with the material's lower crystallinity, concomitant with increased free volume and dye mobility, and is consistent with the optical microscopy study, which revealed the presence of larger aggregates.

## Conclusion

We demonstrated the fabrication of mechanochromic sensors comprised of cyano-OPVs contained in fluorinated polymer matrices. In agreement with previous findings, aggregate size and matrix crystallinity were shown to be important factors determining sensor performance. The formation of sub-micron sized dye aggregates is crucial, since the deformation-induced dispersibility decreases with increase in aggregate size. The present study revealed a surprising difference between the characteristics of cyano-OPVs and fluoropolymers on the one hand and polyolefins on the other. C18-RG, featuring long alkyl tails, provided a superior mechanochromic response in PE matrices in comparison to C1-RG. This was explained with the higher nucleation rate of C18-RG, leading to smaller dye aggregates. Quite surprisingly, the behavior of the two dyes in the presently studied fluoropolymers is essentially opposite: all blends containing C18-RG featured large dye aggregates and displayed no mechanochromic response, in contrast to the C1-RG containing fluoropolymers, in which dye aggregates are smaller and the mechanochromic response is pronounced. This suggests that the nucleation of the luminogenic cyano-OPVs investigated is not intrinsic to the dyes, but is largely governed by the polymer host into which they are embedded. The mechanochromic fluoropolymer/C1-RG blends display a pronounced color change upon deformation. In situ opto-mechanical measurements have shown that the mechanochromic effect occurs primarily during plastic deformation and that the mechanically induced dispersion of the dye aggregates becomes more pronounced as the crystallinity of the matrix polymer increases. These findings correlate with previous work in polyolefin matrices, and show that the underlying mechanism—dispersion of small aggregates of the excimer-forming sensor molecules upon plastic deformation of polymer crystallites—can be exploited in a range of semi-crystalline polymer hosts.

Acknowledgements: This material is based upon work funded by the *National Science Foundation* (NSF DMR-0423914, Center for Layered Polymer Systems at Case Western Reserve University). We acknowledge stimulating discussions with and technical assistance from Dr. J. Kunzelman, Dr. S. Howell, Dr. M. Gawryla, and Dr. L. Tang.

Keywords: luminescence; mechanochromic; sensors

- [1] C. Kocher, P. Smith, C. Weder, *J. Mater. Chem.* **2002**, *12*, 2620.
- [2] M. Burnworth, J. D. Mendez, M. Schroetert, S. J. Rowan, C. Weder, *Macromolecules* **2008**, *41*, 2157.
- [3] K. D. Singer, T. Kazmierczak, J. Lott, H. Song, Y. H. Wu, J. Andrews, E. Baer, A. Hiltner, C. Weder, *Opt. Express* **2008**, *16*, 10358.
- [4] D. Knapton, M. Burnworth, S. J. Rowan, C. Weder, *Angew. Chem., Int. Ed.* **2006**, *45*, 5825.
- [5] B. Z. Tang, *Macromol. Chem. Phys.* **2009**, *210*, 900.
- [6] US 7,223,988 (2007), to Case Western Reserve University, invs.: C. Löwe, C. Weder, Photoluminescent Polymer Blends and Uses Therefore.
- [7] C. L. Li, S. J. Shieh, S. C. Lin, R. S. Liu, *Org. Lett.* **2003**, *5*, 1131.
- [8] F. Z. Henari, H. Manaa, K. P. Kretsch, W. J. Blau, H. Rost, S. Pfeiffer, A. Teuschel, H. Tillmann, H. H. Hörhold, *Chem. Phys. Lett.* **1999**, *307*, 163.
- [9] D. A. M. Egbe, B. Carbonnier, L. M. Ding, D. Muhlbacher, E. Bircckner, T. Pakula, F. E. Karasz, U. W. Grummt, *Macromolecules* **2004**, *37*, 7451.
- [10] B. K. An, S. H. Gihm, J. W. Chung, C. R. Park, S. K. Kwon, S. Y. Park, *J. Am. Chem. Soc.* **2009**, *131*, 3950.
- [11] S. J. Chung, M. Rumi, V. Alain, S. Barlow, J. W. Perry, S. R. Marder, *J. Am. Chem. Soc.* **2005**, *127*, 10844.
- [12] M. Irie, *Chem. Rev.* **2000**, *100*, 1685.
- [13] B. R. Crenshaw, C. Weder, *Adv. Mater.* **2005**, *17*, 1471.
- [14] J. Kunzelman, B. R. Crenshaw, M. Kinami, C. Weder, *Macromol. Rapid Commun.* **2006**, *27*, 1981.
- [15] M. Kinami, B. R. Crenshaw, C. Weder, *Chem. Mater.* **2006**, *18*, 946.
- [16] B. R. Crenshaw, J. Kunzelman, C. E. Sing, C. Ander, C. Weder, *Macromol. Chem. Phys.* **2007**, *208*, 572.
- [17] C. E. Sing, J. Kunzelman, C. Weder, *J. Mater. Chem.* **2009**, *19*, 104.
- [18] J. Kunzelman, B. R. Crenshaw, C. Weder, *J. Mater. Chem.* **2007**, *17*, 2989.
- [19] L. Tang, J. Whalen, G. Schutte, C. Weder, *ACS Appl. Mater. Interfaces* **2009**, *1*, 688.
- [20] C. Lowe, C. Weder, *Adv. Mater.* **2002**, *14*, 1625.
- [21] B. R. Crenshaw, C. Weder, *Chem. Mater.* **2003**, *15*, 4717.
- [22] B. R. Crenshaw, C. Weder, *Macromolecules* **2006**, *39*, 9581.
- [23] B. R. Crenshaw, M. Burnworth, D. Khariwala, A. Hiltner, P. T. Mather, R. Simha, C. Weder, *Macromolecules* **2007**, *40*, 2400.
- [24] J. Kunzelman, M. Gupta, B. R. Crenshaw, D. A. Schiraldi, C. Weder, *Macromol. Mater. Eng.* **2009**, *294*, 244.
- [25] J. Kunzelman, T. Chung, P. T. Mather, C. Weder, *J. Mater. Chem.* **2008**, *18*, 1082.
- [26] A. Pucci, T. Biver, G. Ruggeri, L. I. Meza, Y. Pang, *Polymer* **2005**, *46*, 11198.
- [27] F. Donati, A. Pucci, C. Cappelli, B. Mennucci, G. Ruggeri, *J. Phys. Chem. B* **2008**, *112*, 3668.
- [28] A. Pucci, M. Boccia, F. Galembeck, C. A. D. P. Leite, N. Tirelli, G. Ruggeri, *React. Funct. Polym.* **2008**, *68*, 1144.
- [29] A. Pucci, F. Di Cuia, F. Signori, G. Ruggeri, *J. Mater. Chem.* **2007**, *17*, 783.
- [30] E. M. Rodak, R. J. Taylor, D. B. Hirsch, L. J. Linley, *J. Test. Eval.* **1994**, *22*, 447.
- [31] C. Löwe, C. Weder, *Synthesis* **2002**, *34*, 1185.
- [32] J. Kunzelman, M. Kinami, B. R. Crenshaw, J. D. Protasiewicz, C. Weder, *Adv. Mater.* **2008**, *20*, 119.